Bulletin of Electrical Engineering and Informatics
Vol. 9, No. 6, December 2020, pp. xx~xx
ISSN: 2302-9285, DOI: 10.11591/eei.v9i6.xxxx

Hardware-in-the-loop based comparative analysis of speed controllers using nonlinear control for two-mass system using induction motor drive fed by voltage source inverter with ideal control performance of stator current

Vo Thanh Ha[1], Nguyen Tung Lam[2], Vo Thu Ha[3]
1 Faculty of Electrical and Electrical Engineering, University of Transport and Communications, Vietnam
2 School of Electrical Engineering, Hanoi University of Science and Technology, Vietnam
3 Faculty of Electrical Engineering, University of Economics - Technology for Industries, Vietnam

Article Info

Article history:

Received Jun x, 20xx
Revised Nov x, 20xx
Accepted Dec x, 20xx

Keywords:

Field oriented control
Backstepping
Speed control
Hardware-in-the-Loop
Flatness-based control

ABSTRACT (10 PT)

A comparative study of speed control performance of an induction motor drive system connecting to a load via a non-rigid shaft. The nonrigidity of the coupling is represented by stiffness and damping coefficients deteriorating speed regulating operations of the system and can be regarded as a two-mass system. In the paper, the ability of flatness based and Backstepping controls in control the two-mass system is verified through comprehensive hardware-in-the-loop experiments and with the assumption of ideal stator current loop performance. Step-by-step control design procedures are given, in addition, system responses with classical PID control are also provided for parallel comparisons.

Corresponding Author:

Nguyen Tung Lam,
School of Electrical Engineering, Hanoi University of Science and Technology, Vietnam.
Email: lam.nguyentung@hust.edu.vn

1. INTRODUCTION

Asynchronous electrical drive system is found in enormous applications and is considered as well-established thank to the advancement in current loop control [1]. However, facing mechanical loads, speed control loop design takes a decisive role, especially when the non-rigidity and backlash of the motor-to-load connection is taken into account [2], [3], [4], and [5]. Flexible coupling phenomenon is studied in [6], the authors develop an elegant control scheme integrated with a state observer for estimating motor and load torques. Brock et al [7] propose a filter accompanied with a neural adaptive controller to eliminate high resonance frequencies. The controlled system is analysed through extensive experiments proving the effectiveness of the proposed solution. For a class of multi-mass electrical drive systems where measurement is not always available, a system parameter identification method is presented in [8]. The authors employ pseudo random binary signal and chirp wave to excite necessary information. The approach might be difficult to apply in a wide range of practical systems. A 2DOF PI control is systematically designed in [9] for a two-mass drive coupled via a toothed belt. The tracking results are compared with 1DOF and 1DOF with feedforward controls confirm that the method exhibits robustness and load torque rejection. Due to flat property of the system, Thomsen et al [10] formulate a flatness based control for a finite stiffness coupling drive system fed by an inverter with speed feedback signal. Backstepping control is developed for a multi-motor system which is vastly found in rewinding systems in [11] suppressing flexible coupling phenomenon in linear speed and tension control system. In order to deal with nonlinear stiffness, the authors in [12] implement adaptive Backstepping to reduce connecting shaft oscillations. However, system stiffness characteristic must be known to carry out the control, this requirement might be very challenging in practice. Recently, a active disturbance rejection control (ADRC) is considered as an alternative to classical PID control, an application of ADRC to two-mass system can be found in [13]. A fuzzy based control for a three-mass system is presented in [14] and [15], where fuzzy term is selected to modify IPD control. Other control approaches can be found in [16]–[22].

In general, there is a lack of comprehensive study on how popular control methods react when applying to two-mass drive system operating in nominal range. In the paper, we carry out a hardware-in-the-loop based comparative analysis of speed responses using Backstepping and flatness-based controls in nominal and field-weakening modes. Initially, we present the two-mass drive system in a view of ideal current loop. Subsequently, PID, backstepping, and flatness control design steps are given in details. Finally, hardware-in-the-loop results of three controls are compared and some important conclusions are drawn.

2. TWO-MASS MODEL SYSTEM WITH IDEAL CONTROL PERFORMANCE OF STATOR

Typical configuration of a two-mass system is shown in Figure.1

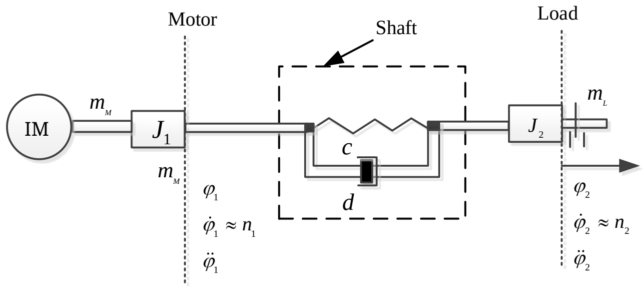

Figure 1. Typical configuration of a two-mass system

When the drive system operates at field weakening range, the mathematical model of the system is [2].

$$\begin{cases} \dfrac{di_{sd}}{dt} = -\left(\dfrac{1}{\sigma T_s} + \dfrac{1-\sigma}{\sigma T_r}\right) i_{sd} + \omega_s i_{sq} + \dfrac{1-\sigma}{\sigma T_r} + \dfrac{1}{\sigma L_s} u_{sd} \\ \dfrac{di_{sq}}{dt} = -\omega_s i_{sd} - \left(\dfrac{1}{\sigma T_s} + \dfrac{1-\sigma}{\sigma T_r}\right) i_{sq} - \dfrac{1-\sigma}{\sigma} \omega i_m + \dfrac{1}{\sigma L_s} u_{sq} \\ \dfrac{d\psi_{rd}}{dt} = -\dfrac{1}{T_r}\psi_{rd} + \dfrac{L_m}{T_r} i_{sd} \\ \dfrac{d\psi_{rq}}{dt} = \dfrac{L_m}{T_r} i_{sq} - (\omega_s - \omega)\psi_{rd} i_{sd} - \dfrac{1}{T_r}\psi_{rq}\dfrac{\psi_{rq}}{L_m} \\ \ddot{\varphi}_1 = -\dfrac{d}{J_1}\dot{\varphi}_1 - \dfrac{c}{J_1}\Delta\varphi + \dfrac{d}{J_1}\dot{\varphi}_2 + \dfrac{1}{J_1} m_M \\ \Delta\dot{\varphi} = \dot{\varphi}_1 - \dot{\varphi}_2 \\ \ddot{\varphi}_2 = \dfrac{d}{J_2}\dot{\varphi}_1 + \dfrac{c}{J_2}\Delta\varphi - \dfrac{d}{J_2}\dot{\varphi}_2 - \dfrac{1}{J_2} m_L \end{cases} \quad (1)$$

In which, $i_{sd}; i_{sq}$ are dq components of the stator current; ω, ω_s are mechanical rotor and synchronous speeds, respectively; ψ'_{rd}, ψ'_{rq} are dq components of the rotor flux ; σ is total leakage factor; T_r is rotor time constant: u_{sd} , u_{sq} are dq components of the stator voltage; L_s is stator inductance, $\dot{\varphi}_1, \dot{\varphi}_2$ are motor and load speeds; $\ddot{\varphi}_1, \ddot{\varphi}_2$ are motor and load angle accelerations; φ is rotor angle; d is shaft damping coefficient; c is shaft stiffness. It can be seen that the original state Eq (1) is bilinear and is of 7th order. Assume that the current controller is perfect with ideal response, the induction motor model can be reduced as in (2).

$$\begin{cases} \dfrac{di_m}{dt} = \dfrac{1}{T_r} i_{sd} - \dfrac{1}{T_r} i_m \\ \ddot{\varphi}_1 = -\dfrac{d}{J_1}\dot{\varphi}_1 - \dfrac{c}{J_1}\Delta\varphi + \dfrac{d}{J_1}\dot{\varphi}_2 + \dfrac{1}{J_1} m_M \\ \Delta\dot{\varphi} = \dot{\varphi}_1 - \dot{\varphi}_2 \\ \ddot{\varphi}_2 = \dfrac{d}{J_2}\dot{\varphi}_1 + \dfrac{c}{J_2}\Delta\varphi - \dfrac{d}{J_2}\dot{\varphi}_2 - \dfrac{1}{J_2} m_L \end{cases} \tag{2}$$

Where: $i_m = \dfrac{\psi_{rd}}{L_m}$. The state Eq. (2) is of 4nd order, stator current i_{sd} is used to control the motor flux and i_{sq} is dedicated to speed control. For control design purpose, Eq. (2) is rewritten in the following state-space form:

$$\begin{bmatrix} i_m \\ \ddot{\varphi}_1 \\ \Delta\dot{\varphi} \\ \ddot{\varphi}_2 \end{bmatrix} = \begin{bmatrix} \dfrac{-1}{T_r} & 0 & 0 & 0 \\ 0 & \dfrac{-d}{J_1} & \dfrac{-c}{J_1} & \dfrac{d}{J_1} \\ 0 & 1 & 0 & -1 \\ 0 & \dfrac{d}{J_2} & \dfrac{c}{J_2} & \dfrac{-d}{J_2} \end{bmatrix} \begin{bmatrix} i_m \\ \dot{\varphi}_1 \\ \Delta\varphi \\ \dot{\varphi}_2 \end{bmatrix} + \begin{bmatrix} \dfrac{1}{T_r} & 0 \\ 0 & \dfrac{k_\omega i_m}{J_1} \\ 0 & 0 \\ 0 & 0 \end{bmatrix} \begin{bmatrix} i_{sd} \\ i_{sq} \end{bmatrix} + \begin{bmatrix} 0 \\ 0 \\ 0 \\ \dfrac{-1}{J_2} \end{bmatrix} m_L \tag{3}$$

Where we have defined

$$y^T = i_m, \dot{\varphi}_2 \; ; \begin{bmatrix} i_m \\ \dot{\varphi}_2 \end{bmatrix} = \begin{bmatrix} 1 & 0 & 0 & 0 \\ 0 & 0 & 0 & 1 \end{bmatrix} \begin{bmatrix} i_m \\ \dot{\varphi}_1 \\ \Delta\varphi \\ \dot{\varphi}_2 \end{bmatrix} \tag{4}$$

3. SPEED CONTROL DESIGN

3.1 PI control

PI controller is designed according to the symmetric optimal standard, so we have the PI control structure shown as Figure. 3. The design of PI for the system is well-established, readers can refer to [23] and [24] for more details.

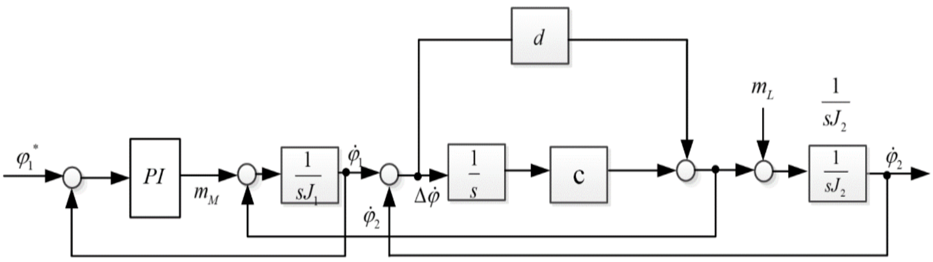

Figure.3: Block diagram of PI control algorithm of a two-mass system

3.2. Backstepping control

For designing step, it is assumed that all feedback signals from the motor, the shaft and the load sides are available. As in Fig. 3, the proposed backstepping control algorithm is designed in two steps. In each step a subsystem will be studied. Each step includes the dynamics of the previous subsystems for backstepping technique. Selecting a proper Lyapunov function for each step, guarantees the asymptotic stability of the related subsystem. Completing all two steps, results in the asymptotic stability of the whole system implying the desired input (motor torque) for accurate load speed control [25].

The speed control equation is given:

$$\begin{cases} \dfrac{d\dot{\varphi}_2}{dt} = -\dfrac{d}{J_2}\dot{\varphi}_2 + \dfrac{c}{J_2}\Delta\varphi + \dfrac{d}{J_2}\dot{\varphi}_1 - \dfrac{1}{J_2} m_L \\ \dfrac{d\dot{\varphi}_1}{dt} = -\dfrac{d}{J_1}\dot{\varphi}_1 - \dfrac{c}{J_1}\Delta\varphi + \dfrac{d}{J_1}\dot{\varphi}_2 - \dfrac{k_\omega . \psi'_{rd}}{J_1} i_{sq} \end{cases} \tag{5}$$

where $m_M = k_\omega (\psi_{rd} / L_m) i_{sq} ; k_\omega = (3/2) z_p (L_m / L_r)$ is motor torque. To be able to apply backstepping control method conveniently, we set:

$$\begin{cases} x_1 = \dot{\varphi}_2 \\ x_2 = \dot{\varphi}_1 \\ u = i_{sq} \\ y = x_1 = \dot{\varphi}_2 \end{cases} \tag{6}$$

Where x_1 and x_2 are state variables; *u* is the control variable and *y* is the output (the load rotating speed). Since then the system is expressed in the form of strict feedback as follows:

$$\begin{cases} \dot{x}_1 = (\frac{d\dot{\varphi}_2}{dt}) = f_1(x_1, x_2) \\ \dot{x}_2 = (\frac{d\dot{\varphi}_1}{dt}) = f_2(x_1, x_2, \mathrm{u}) \\ y = x_1 = \dot{\varphi}_2 \end{cases} \tag{7}$$

To implement backstepping control we define:

$$\begin{cases} z_1 = x_1 - x_{1d} = \dot{\varphi}_2 - \dot{\varphi}_{2d} \\ z_2 = x_2 - x_{2dka} = \dot{\varphi}_1 - \dot{\varphi}_{1dka} \end{cases} \tag{8}$$

Where $x_{1d} = \dot{\varphi}_{2d}$ is the set value of the output variable and $x_{2dka} = \dot{\varphi}_{1dka}$ is the virtual control. Selecting the Lyapunov candidate function as follows:

$$V_1 = \frac{1}{2} z_1^2 \tag{9}$$

Taking derivative of eq.(9) results in:

$$\dot{V}_1 = z_1 \dot{z}_1 \tag{10}$$

Because of $\ddot{\varphi}_{1d} = 0$ so that eq.(8) rendered as $\dot{z}_1 = \ddot{\varphi}_2$, substitution $\dot{z}_1$ from eq.(5) into eq.(10) yields:

$$\dot{V}_1 = z_1 \left[-k_1 z_1 + \frac{d}{J_2}\dot{\varphi}_1 + (k_1 z_1 + \frac{c}{J_2}\Delta\varphi - \frac{1}{J_2} m_L - \frac{d}{J_2}\dot{\varphi}_2) \right] \tag{11}$$

Considering $\dot{\varphi}_1$ as the virtual control variable in such a way that $\dot{\varphi}_1 = \dot{\varphi}_{1dka}$ so that:

$$\frac{d}{J_2}\dot{\varphi}_{1dka} = -(k_1 z_1 + \frac{c}{J_2}\Delta\varphi - \frac{1}{J_2} m_L - \frac{d}{J_2}\dot{\varphi}_2) \tag{12}$$

If $\dot{V}_1 = -k_1 z_1^2 < 0$, with $\forall k_1 > 0$ then the stable condition is satisfied. Defining:

$$B_f = \frac{c}{J_2}\Delta\varphi - \frac{1}{J_2} m_L - \frac{d}{J_2}\dot{\varphi}_2 \tag{13}$$

Substitution of eq.(13) into eq.(12) results in:

$$\dot{\varphi}_{1dka} = -\frac{J_2}{d}[k_1 z_1 + B_f] \tag{14}$$

The control specified in eq(14) ensures that the load speed tracks the desired value. Next, the control for the motor side is designed. It is noted that $x_{1d} = \dot{\varphi}_{2d}$ is constant, so that from eq.(5) and eq.(8) and eq. (13) can be shortened as:

$$\dot{z}_1 = \frac{d\dot{\varphi}_2}{dt} = \ddot{\varphi}_2 = \frac{d}{J_2}\dot{\varphi}_1 + B_f \tag{15}$$

Select the Lyapunov candidate function as follows:

$$V_2 = V_1 + \frac{1}{2} z_2^2 \tag{16}$$

Taking derivative of eq.(16) gives:

$$\dot{V}_2 = \dot{V}_1 + z_2 \dot{z}_2 \tag{17}$$

From eq.(11) and eq.(12), we can write as:

$$\dot{V}_2 = -k_1 \dot{z}_1^2 + \frac{d}{J_2} z_1 (\dot{\varphi}_1 - \dot{\varphi}_{1dka}) + z_2 \dot{z}_2 \tag{18}$$

After some basic operations, it can be shown that

$$\dot{V}_2 = -k_1\dot{z}_1^2 - k_2 z_2^2 + k_2 z_2^2 + \frac{d}{J_2} z_1(\dot{\varphi}_1 - \dot{\varphi}_{1dka}) + z_2\dot{z}_2 \tag{19}$$

Where we have defined $\dot{\varphi}_1 - \dot{\varphi}_{1dka} = z_2$, so that:

$$\dot{V}_2 = -k_1 z_1^2 - k_2 z_2^2 + z_2(k_2 z_2 + \frac{d}{J_2} z_1 + \dot{z}_2) \tag{20}$$

At this point in order to render $\dot{V}_2 < 0$, the following conditions must be fullfied:

$$k_2 > 0 \text{ and } k_2 z_2 + \frac{d}{J_2} z_1 + \dot{z}_2 = 0 \tag{21}$$

Conditions specified in Eq. (21) imply that

$$\ddot{\varphi}_1 - \ddot{\varphi}_{1dka} = -k_2(\dot{\varphi}_1 - \dot{\varphi}_{1dka}) - \frac{d}{J_2} z_1 \tag{22}$$

From eq.(14), it indicates that

$$\ddot{\varphi}_{1dka} = -\frac{J_2}{d}(k_1\dot{z}_1 + \dot{B}_f) \text{ and } \dot{\varphi} - \dot{\varphi}_{1dka} = \dot{\varphi}_1 + \frac{J_2}{d}(k_1 z_1 + B_f) \tag{23}$$

Substituting eq.(15) and eq.(22) into eq.(23) gives:

$$\ddot{\varphi}_1 = -(k_1 + k_2)\dot{\varphi}_1 - (\frac{J_2}{d}k_1k_2 + \frac{J_2}{d})z_1 - \frac{J_2}{d}(k_1 + k_2)B_f - \frac{J_2}{d}\dot{B}_f \tag{24}$$

To proceed to calculate the final expression of the control current, first of all, we substitution from the second equation of the system eq.(5) into eq.(24) we have:

$$\frac{k_\omega \psi'_{rd}}{J_1}.i_{sq} = [\frac{d}{J_1} - (k_1 + k_2)]\dot{\varphi}_1 - \frac{d}{J_1}\dot{\varphi}_2 + \frac{c}{J_1}\Delta\varphi - (\frac{J_2}{d}k_1k_2 + \frac{d}{J_2})z_1 - \frac{J_2}{d}(k_1 + k_2)B_f - \frac{J_2}{d}\dot{B}_f \tag{25}$$

From the expression eq. (25) and using fundamental calculation, we will get the final expression of i_{sq} is:

$$i_{sq} = \frac{J_1}{k_\omega \psi'_{rd}} \left\{ \begin{array}{c} [\frac{d}{J_1} + \frac{d}{J_2} - (\frac{c}{d} + k_1 + k_2)](\dot{\varphi}_1 - \dot{\varphi}_2) + [\frac{c}{J_1} + \frac{c}{J_2} - \frac{c}{d}(k_1 + k_2)]\Delta\varphi \\ -(\frac{J_2}{d}k_1k_2 + \frac{d}{J_2})(\dot{\varphi}_2 - \dot{\varphi}_{2d}) + \frac{m_w}{d}(k_1 + k_2 - \frac{d}{J_2}) \end{array} \right\} \tag{26}$$

Based on eq.(26), the proposed control scheme for the two-mass system using induction motor fed by VSI with perfect stator current controller is shown in Fig. 4.

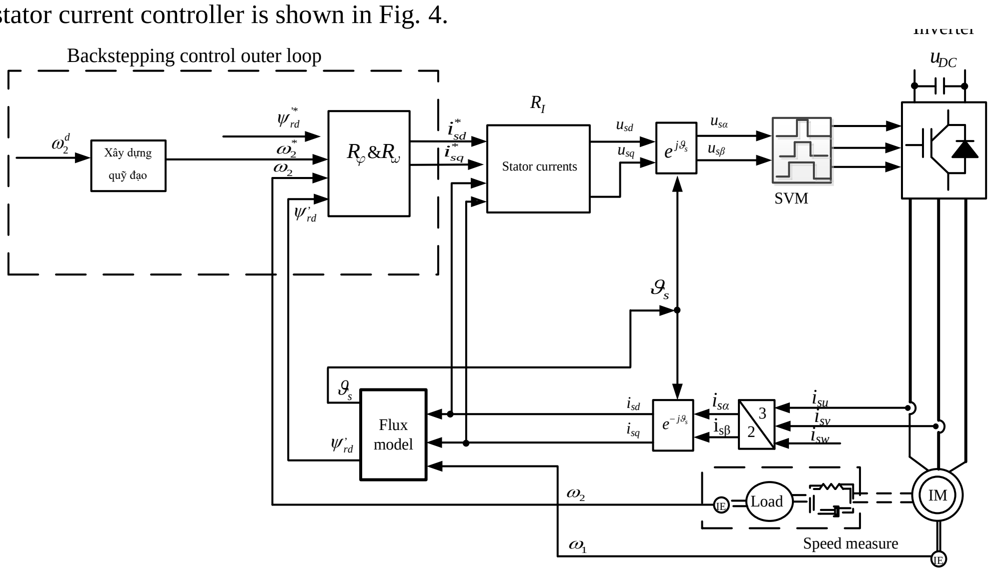

Figure.4: Block diagram of backstepping control algorithm of a two-mass system

3.3. Flatness-based control (FBC)

3.3.1 Feedforward control design

Feedforward control is indeed the inverse mathematical model of the control plant and plays a key role in the FBC structure. From Eq.(5), the feedforward controller can be deduced as

$$\begin{cases} i_{sd}^{ff} = i_m^* + T_r \dfrac{di_m^*}{dt} \\ i^{ff}{}_{sq} = \dfrac{J_1\ddot{\varphi}_1 + J_2\ddot{\varphi}_2 + m_L}{k_\omega i^*{}_m} \end{cases} \tag{27}$$

Based on equation $\ddot{\varphi}_1 = -\frac{J_2}{J_1}\ddot{\varphi}_2 + \frac{1}{J_1}\ m_M - m_L$ [26], it can be deduced that:

$$J_1\dot{\omega}_1 + J_2\dot{\omega}_2 = m_M - m_L \tag{28}$$

Assume that the load torque is constant, then the load observer can be designed as:

$$\begin{cases} \dfrac{d m_L}{dt} = -l_1\ \ \omega_2 - \omega_2 \\ \dfrac{d\omega_2}{dt} = \dfrac{1}{J_2}\ \ m_M - m_L - J_1\dot{\omega}_1\ \ + l_2\ \ \omega_2 - \omega_2 \end{cases} \tag{29}$$

where $m_M = k_\omega i_m i_{sq}$. then from Eq.(29) and Eq. (28), it is straightforward to show that

$$\begin{cases} \dfrac{d\ \ m_L - m_L}{dt} = -l_1\ \ \omega_L - \omega_L \\ \dfrac{d\ \ \omega_L - \omega_L}{dt} = -\dfrac{1}{J_2}\ \ m_L - m_L + J_1\dot{\omega}_M - J_1\dot{\omega}_M\ \ + l_2\ \ \omega_L - \omega_L \end{cases} \tag{30}$$

Defineing $\varepsilon_m = m_L - m_L$; $\varepsilon_\omega = \omega_L - \omega_L$ and substituting into Eq.(30) give

$$\begin{cases} \dfrac{d\varepsilon_m}{dt} = -l_1\varepsilon_\omega \\ \dfrac{d\varepsilon_\omega}{dt} = -\dfrac{1}{J_2}\varepsilon_m + l_2\varepsilon_\omega + f\ \ \dot{\omega}_M, \dot{\omega}_M \end{cases} \tag{31}$$

The error model is

$$\begin{bmatrix} \dfrac{d\varepsilon_m}{dt} \\ \dfrac{d\varepsilon_\omega}{dt} \end{bmatrix} = \begin{bmatrix} 0 & -l_1 \\ -\dfrac{1}{J_2} & l_2 \end{bmatrix} \begin{bmatrix} \varepsilon_m \\ \varepsilon_\omega \end{bmatrix} + \begin{bmatrix} 0 \\ f\ \ \dot{\omega}_M, \dot{\omega}_M \end{bmatrix} \tag{32}$$

The characteristic equation of Eq.(32) is

$$\det\ s\mathbf{I} - \mathbf{A}\ = s^2 - l_2 s - \frac{l_1}{J_2} = 0 \tag{33}$$

By selecting l_1 and l_2 such that:

$$l_1 = -J_2 s_1 s_2 ; l_2 = s_1 + s_2 \tag{34}$$

3.3.2 Design of the reference trajectories

The equation $\mathbf{x} = P\left(\mathbf{y}, \frac{d\mathbf{y}}{dt}, \ldots, \frac{d^r\mathbf{y}}{dt^r}\right)$; $r \in N; \mathbf{u} = Q\left(\mathbf{y}, \frac{d\mathbf{y}}{dt}, \ldots, \frac{d^{(r+1)}\mathbf{y}}{dt^{(r+1)}}\right)$ is also called the "inverse" process model of the system corresponding to the output given in equation $\mathbf{y} = \begin{bmatrix} y_1 \\ \vdots \\ y_m \end{bmatrix} = F\left(\mathbf{x}, \mathbf{u}, \frac{d\mathbf{u}}{dt}, \ldots, \frac{d^l\mathbf{u}}{dt^l}\right)$; $l \in N$. So that, it can be concluded that to every output trajectory $t \to \mathbf{y}(t)$ being enough differentiable there corresponds a state and input trajectory that identically satisfies the system equations. This FBC structure for two-mass system is built resulting from acceptance of the trajectory. That mean reference available must also be enough differentiable output. Thus the control structure is extended by a block which plays the role of setting the trajectory for reference available.

Flux reference trajectories

a. *Trajectories of flux reference*:

$$i_m^* + 2T_1\frac{di_m^*}{dt} + T_1^2\frac{d^2 i_m^*}{dt^2} = i_m^d \Leftrightarrow \frac{d^2 i_m^*}{dt^2} = \frac{1}{T_1^2}\left(i_m^d - i_m^* - 2T_1\frac{di_m^*}{dt}\right) \tag{35}$$

b. Speed reference trajectories

Trajectories of speed reference is given as:

$$\omega^*(t) = \begin{cases} \omega_0 + a_{11}t + a_{21}t^2 + a_{31}t^3 + a_{41}t^4 & 0 \le t \le 2t_0 \\ \omega_0 + At_0 + A(t-2t_0) & 2t_0 < t \le t_E - 2t_0 \\ a_{02} + a_{12}\tau + a_{22}\tau^2 + a_{32}\tau^3 + a_{42}\tau^4 & t_E - 2t_0 < t \le t_E \end{cases} \quad (36)$$

Where:

$$A = \frac{\omega_E - \omega_0}{t_E - 2t_0}\,;\ \tau = t - (t_c - 2t_0)\,;\ a_{11} = a_{21} = 0\,;\ a_{31} = \frac{1}{4t_0^2}A\,;\ a_{41} = -\frac{1}{16t_0^3}A$$

3.3.3 Feedback control design

To handle the flux and the speed of the motor, the well-known PI controller is chosen. The detail equations of the flux and speed controller are described by Eq. (29) and Eq. (30), respectively

$$R_\psi = V_\psi \frac{1 + d_\psi z^{-1}}{1 - z^{-1}}\ with\ V_\psi \approx \frac{1}{3\left(1 - e^{-T_\psi/T_r}\right)}\,;d_\psi \approx e^{-T_\psi/T_r} \quad (37)$$

$$\Delta i_{sq} = \frac{J_1 J_2 \Delta\dddot{\omega}_2 + (dJ_1 + dJ_2)\Delta\ddot{\omega}_2}{k_\omega i_m ac} + \frac{(J_1 c + J_2 ac)\Delta\dot{\omega}_2}{k_\omega i_m ac} \quad (38)$$

Where: $\Delta i_{sq} = i_{sq}^* - i_{sq}^{*ff}$; $\Delta\omega_2 = \omega_2 - \omega_2^*$. Laplace transform of Eq.(38) provides the transfer function of error speed and flux:

$$\frac{\Delta\omega_2(s)}{\Delta i_{sq}(s)} = \frac{k_\omega i_m ac}{s\left[J_1 J_2 s^2 + (dJ_1 + dJ_2)s + cJ_1 + acJ_2\right]} \quad (39)$$

Based on feedforward and feedback control design and trajectories of speed and flux reference the proposed control scheme for the two-mass system using induction motor fed by VSI with perfect stator current controller is shown in Figure. 5.

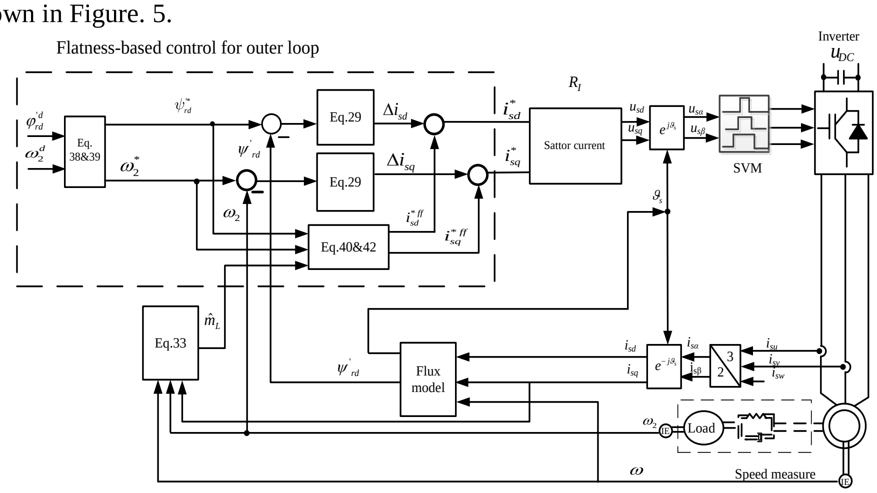

Figure. 5 Block diagram fltaness based control of two-mass system

4. RESULT AND DISCUSSION

In this section, the proposed control strategy is verified by simulation using Hardware-in-the-Loop (HIL). The system hardware is simulated in real time on the HIL platform with a time step of 1 μs that means very close to physical models, while the pulse width modulation (PWM) carrier frequency is 5 kHz. Voltage and current controllers are implemented in DSP TMS320F2808. The simulation parameters are: rated power=2.2kW; rated phase voltage=380/220VRMS; rated frequency= 50Hz; d=0.015Nm/rad; c=0.28Nm/rad, J1 = 7.455x10-5Kgm2; J2 = 5.5913x10-5Kgm2; with load moment is 1.5Nm.

Simulation procedure is as follows: At t = 0s, the magnetic current is created. Then at time instance t = 0.5s, the motor starts to speed up to 1000rpm and 1rpm. At t=2s, the reverse speed, the motor starts to speed downd to -1000rpm and -1rpm. At t=4s, stop system. This section provides evaluation of HIL simulation results that speed response. The evaluation of the speed control for two-mass system, is shown in Figure 7, Table 1.

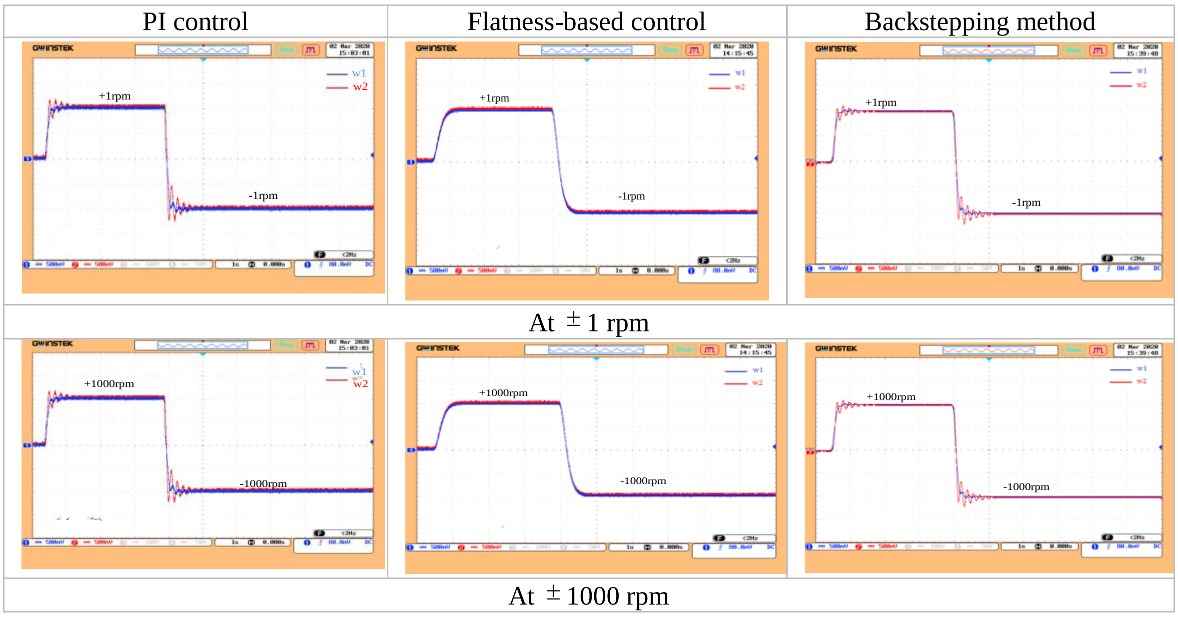

Figure. 7 Speed response of Simulation/HIL platform at ± 1rmp and ± 1000 rmp

Table 1. HIL test results of the speed controls

Speed control	Deadbeat PI	Deadbeat Backstepping	Deadbeat Flatness
At the speed of ± 1 rpm			
Accelerating time (s)	50	50	0
Speed settling time (s)	2.5	2.0	1.0
At the speed of ± 1000 rpm			
Accelerating time (s)	50	50	0
Speed settling time (s)	3.0	2.5	1.0

It is found that the nonlinear control method based on the flatness-based control principle gives better than the PI controller and backstepping method results, as the referened load speed match with motor speed after a short period of time (0.3 seconds at (±) 1rpm and 0.5 seconds at (±) 1000rpm (at up and reverse speed), without overshoot. That implies the speed controller based on the flatness-based control, which suppressed resonance oscillation over the entire operating range of the IM motor.

From the results, we know that the two-mass system with flexible couplings when operating at the speed of (±)1000rpm and even at the low speed range (±) 1rpm, the nonlinear control method, based on the flatness-based control, has proved its advantage by solving the problem of resonant vibration suppression at the spindle compared to the PI controller and backstepping. Besides of at times of transition with fast setting time, without overshoot and load speed matcht with motor speed.

In the following simulation scenario, the motor is set in field-weakening region. The system responses of magnetizing current are shown in Fig. 8 and Fig. 9. The three control methods show stable operation not only in nominal but also field weakening range. However, it can be observed that the flatness-based control gives better transient response, i.e., without overshoot as seen in Figure.9 and shorter settling time (0.2s in comparison with 0.5s for PI control and backstepping method).

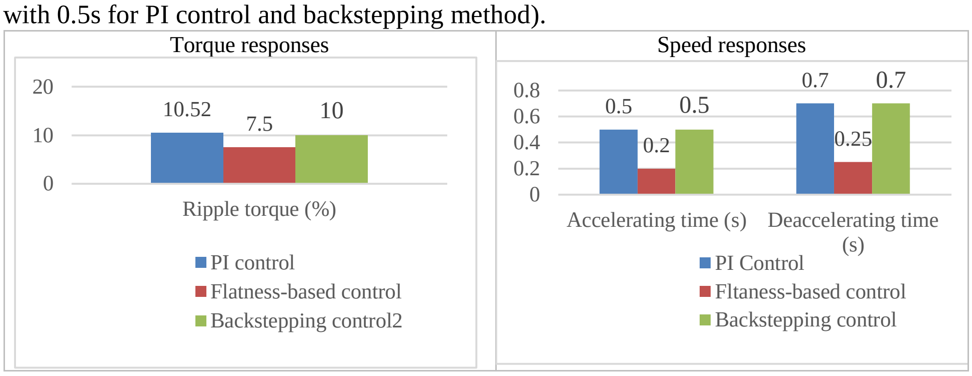

Figure 8: Chart of torque and speed responses

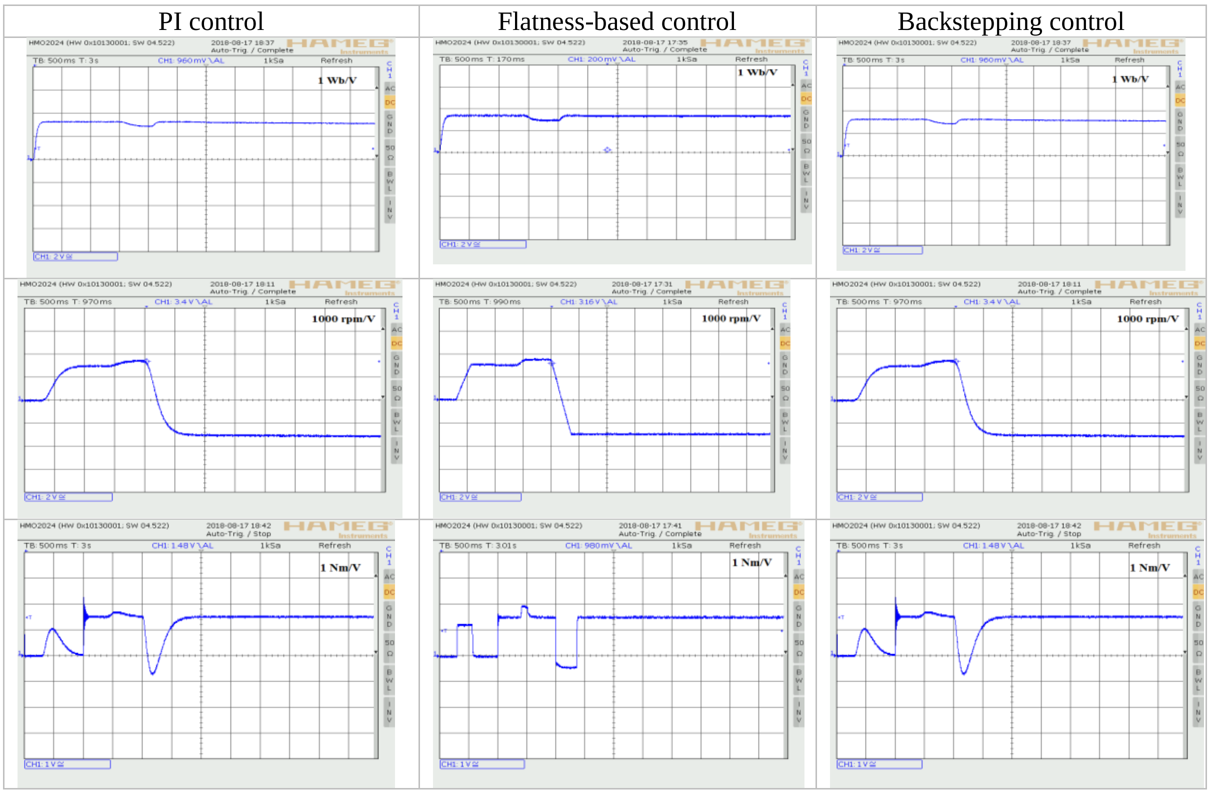

Figure 9*:* Flux, speed and torque responses

5. CONCLUSION

In this paper, the two-mass system with flexible couplings comprises of an induction motor and a load is considered. At the motor side, the current response is assumed to be ideal leading to a simplified model. PI control, Flatness-based control, and backstepping control are employed to solve flux and speed control problem of the system. The HIL based test shows better control performances of flatness control compared to the other two schemes. This conclusion implies possibility of practical uses of flatness control in dealing with systems with flexible couplings. In the future reseach, in order to give a concrete evaluation, roburstnees experiments against varying system parameter and load disturbances will be carried out.

REFERENCES

[1] V. T. Ha, N. T. Lam, V. T. Ha, and V. Q. Vinh, “Advanced control structures for induction motors with ideal current loop response using field oriented control,” *Int. J. Power Electron. Drive Syst.*, vol. 10, no. 4, pp. 1758–1771, 2019.

[2] D. Łuczak, “Mathematical model of multi-mass electric drive system with flexible connection,” *2014 19th Int. Conf. Methods Model. Autom. Robot. MMAR 2014*, pp. 590–595, 2014.

[3] C. Ma and Y. Hori, “Backlash Vibration Suppression Control of Torsional System by Novel Fractional Order PIDk Controller,” *IEEJ Trans. Ind. Appl.*, vol. 124, no. 3, pp. 312–317, 2004.

[4] P. J. Serkies and K. Szabat, “Model predictive control of the two-mass with mechanical backlash,” *Comput. Appl. Electr. Eng.*, pp. 170–180.

[5] M. Mola, A. Khayatian, and M. Dehghani, “Backstepping position control of two-mass systems with unknown backlash,” *2013 9th Asian Control Conf. ASCC 2013*, 2013.

[6] J. Vittek, V. Vavrúš, P. Briš, and L. Gorel, “Forced Dynamics Control of the Elastic Joint Drive with Single Rotor Position Sensor,” *Autom. – J. Control. Meas. Electron. Comput. Commun.*, vol. 54, no. 3, pp. 337–347, 2013.

[7] S. Brock, D. Zuczak, K. Nowopolski, T. Pajchrowski, and K. Zawirski, “Two Approaches to Speed Control for Multi-Mass System With Variable Mechanical Parameters,” *IEEE Trans. Ind. Electron.*, vol. 64, no. 4, pp. 3338–3347, 2017.

[8] J. Rigelsford, “Intelligent Observer and Control Design for Nonlinear Systems,” *Ind. Robot An Int. J.*, vol. 27, no. 4, 2000.

[9] S. E. Saarakkala, M. Hinkkanen, and K. Zenger, “Speed control of two-mass mechanical loads in electric drives,” *2012 IEEE Energy Convers. Congr. Expo. ECCE 2012*, no. June 2016, pp. 1246–1253, 2012.

[10] S. Thomsen and F. W. Fuchs, “Flatness based speed control of drive systems with resonant loads,” *IECON Proc. (Industrial Electron. Conf.*, pp. 120–125, 2010.
[11] L. T. Thi, L. N. Tung, C. Duc Thanh, D. N. Quang, and Q. N. Van, “Tension regulation of roll-To-roll systems with flexible couplings,” in *Proceedings of 2019 International Conference on System Science and Engineering, ICSSE 2019*, 2019, pp. 441–444.
[12] J. KABZIŃSKI, “Adaptive Control of Two-Mass Drive System with Nonlinear Stiffness,” *Przegląd Elektrotechniczny*, vol. 1, no. 3, pp. 51–56, 2018.
[13] S. Zhao and Z. Gao, “An active disturbance rejection based approach to vibration suppression in two-inertia systems,” *Asian J. Control*, vol. 15, no. 2, pp. 350–362, 2013.
[14] H. Ikeda, T. Hanamoto, T. Tsuji, and M. Tomizuka, “Design of vibration suppression controller for 3-inertia system using Taguchi Method,” *Int. Symp. Power Electron. Electr. Drives, Autom. Motion, 2006. SPEEDAM 2006*, vol. 2006, no. 3, pp. 1045–1050, 2006.
[15] H. Ikeda and T. Hanamoto, “Fuzzy controller of multi-inertia resonance system designed by Differential Evolution,” *2013 Int. Conf. Electr. Mach. Syst. ICEMS 2013*, vol. 3, no. 2, pp. 2291–2295, 2013.
[16] R. Zhang and C. Tong, “Torsional vibration control of the main drive system of a rolling mill based on an extended state observer and linear quadratic control,” *JVC/Journal Vib. Control*, vol. 12, no. 3, pp. 313–327, 2006.
[17] Y. Hori, H. Sawada, and Y. Chun, “Slow resonance ratio control for vibration suppression and disturbance rejection in torsional system,” *IEEE Trans. Ind. Electron.*, vol. 46, no. 1, pp. 162–168, 1999.
[18] D. Luczak, P. Siwek, and K. Nowopolski, “Speed controller for four-mass mechanical system with two drive units,” *Proc. - 2015 IEEE 2nd Int. Conf. Cybern. CYBCONF 2015*, pp. 449–454, 2015.
[19] M. Valásek, “Design of Nonlinear Control of Nonlinear Multibody Systems,” in *Virtual Nonlinear Multibody Systems*, 2003, vol. 103, pp. 263–278.
[20] K. Nowopolski, B. Wicher, D. Łuczak, and P. Siwek, “Recursive neural network as speed controller for two-sided electrical drive with complex mechanical structure,” *2017 22nd Int. Conf. Methods Model. Autom. Robot. MMAR 2017*, pp. 576–581, 2017.
[21] K. T. Nam, S. J. Lee, T. Y. Kuc, and H. Kim, “Position and velocity estimation for two-inertia system with nonlinear stiffness based on acceleration sensor,” *Sensors (Switzerland)*, vol. 16, no. 1, pp. 1–10, 2016.
[22] P. Serkies, “Piotr Serkies Comparison of the control methods of electrical drives with an elastic coupling allowing to limit the torsional torque amplitude Porównanie metod sterowania napędem elektrycznym z połączeniem sprężystym pozwalające na ograniczenie amplitudy ,” vol. 19, no. 2, pp. 203–210, 2017.
[23] Zhang G and Furusho J, “Speed Control of Two-Inertia System by PI/PID Control,” *IEEE Trans. Ind. Electron.*, vol. 47, no. 3, pp. 603–609, 2000.
[24] K. S. and T. Orlowska-Kowalska, “Vibration suppression in a two-mass drive system using PI speed controller and additional feedbacks - comparative study,” *IEEE Trans. Ind. Electron.*, vol. 54, no. 2, pp. 1193–1206, 2007.
[25] N. P. Q. Vo Thanh Ha, Le Trong Tan, Nguyen Duc Nam, “Backstepping Control of Two-Mass System Using Induction Motor Drive Fed by Voltage Source Inverter with Ideal Control Performance of Stator Current,” *Int. J. Power Electron. Drive Syst.*, vol. 10, no. 2, pp. 720–730, 2019.
[26] N. P. Q. Vo Thanh Ha, L “Flatness-Based Control Design for Two-Mass System Using Induction Motor Drive Fed by Voltage Source Inverter with Ideal Control Performance of Stator Current,” *Proceedings of the VIII International Conference of Students, PhD Students and Young Scientists, May, 16, 2019. Mechanisms and Machine Science 70, Mechanisms and Machine Science, ISBN 978-3-030-13321-4 (eBook),* https://doi.org/10.1007/978-3-030-13321-4, pp39-50, Springer Nature Switzerland, *2019*.

BIOGRAPHIES OF AUTHORS

Vo Thanh Ha received the B.S degree in Control and Automation Engineering from Thai Nguyen University of Technology, Vietnam in 2002, the Master’s degree from Hanoi University of Science and Technology, Vietnam in 2004 and she received the Ph. D degree from Hanoi University of Science and Technology, Viet Nam in 2020, both in Control and Automation Engineering. She has worked in University of Transport and Communication, as a lecturer since 2005. Her current areas of research are electrical drive and power electronics.

	Nguyen Tung Lam received the B.S degree in Control and Automation Engineering from Hanoi University of Science and Technology, Hanoi, Vietnam, 2005, the M.S degree from Asian Institute of Technology, 2007, and the Ph. D from The University of Western Australia, 2014. He is current working as a lecturer at Department of Industrial Automation, School of Electrical Engineering, Hanoi University of Science and Technology. His research interests include motion control, control system and its applications. Currently, Dr Nguyen′s research activities target to motion control including active magnetic bearings, rewinding systems, dual-arm robots, and power assist systems.
	Vo Thu Ha received the B.S degree in Control and Automation Engineering from Thai Nguyen University of Technology, Vietnam in 2002, the Master’s degree from Hanoi University of Science and Technology, Vietnam in 2004, and the Ph. D from Hanoi University of Science and Technology, Vietnam in 2012. She received the Assoc. Prof. degree in automation engineering from University of Economics - Technology for Industries in 11/2017. She has worked in Faculty of Electrical Engineering, University of Economics - Technology for Industries since 2003, Vietnam. Assoc. Prof Vo Thu Ha′s research are robot control, electrical drive, power electronics, modeling and simulation.